2018 IEEE Intelligent Vehicles Symposium (IV)
Changshu, Suzhou, China, June 26-30, 2018

Adaptive Multivariable Super-Twisting Control for Lane Keeping of Autonomous Vehicles with Differential Steering

Chuan Hu[1], Rongrong Wang[2] and Yechen Qin[3*]

Abstract— **This paper investigates the lane keeping control for four-wheel independently actuated autonomous vehicles. To guarantee the vehicle safety when the active-steering motor entirely fails, the steering manoeuvre is accomplished by the differential drive assisted steering (DDAS), which is generated by the differential moment between the front wheels. A novel adaptive multivariable super-twisting control strategy is proposed to realize the control objective in finite time, considering the multiple unknown and mismatched disturbances of the steering system with the chattering effect removed. In the sliding surface, a nonlinear function is designed to adaptively change the damping ratio of the closed-loop system so as to improve the transient performance of the lane keeping control in the faulty condition. The finite-time convergence of the closed-loop system is proved by Lyapunov function technique. Results of CarSim-Simulink simulations with a high-fidelity and full-car model have verified the effectiveness and robustness of the proposed controller in the lane keeping control with DDAS and guaranteeing high performance.**

I. INTRODUCTION

Complex modern transportation environments and changing urban traffic conditions have set up high requirements for autonomous vehicles (AV), which has driven AV research to increase the transportation safety, efficiency and reliability [1]. In this sense, the vehicle fault-tolerant control will be of great importance and necessity in vehicular cyber-physical system design. The rapid development and research of electric vehicles [2]–[7] have yielded great promotion in the advancement of AVs. In the field of vehicle actuators, the emerging four-wheel independent actuations provide great potentials in improving the vehicle control redundancy, flexibility and maneuverability [8]. The mounted in-wheel motors can generate accurate and fast torque response, yielding better performance and control efficiency especially when the vehicle is driving near the handling limit or in adverse conditions. Thus independently actuated (IA) AVs will obtain higher performance, reliability and safety [9]–[11].

The lane keeping is an important issue of the advanced driver assistance systems (ADAS) in the development of AVs. The lane departure will be more likely to be caused by the faults of the vehicle control system or actuators for AVs. Therein, the failure of the active front-wheel steering (AFS) system is a highly dangerous failure type, easily leading to serious accidents. On this occasion, this paper investigates the lane keeping control of four-wheel independently actuated (FWIA) AVs when the steering motor completely fails, by using the external front differential moment to generate a differential drive assisted steering (DDAS) angle [12] in the presence of the nonzero scrub radius in the steering system. Few previous literature investigated the vehicle yaw control using DDAS mechanism [13], and they usually regarded the differential drive as an assistance steering power to alleviate the driver's steering effort. Also, the transient performance improvement in this transition was less researched before, as the time-consuming fault diagnosis and control switching may deteriorate the control performance [14].

Sliding mode control (SMC) is a widely used control approach in the vehicle motion control scenarios which involve various external disturbances [15], [16]. To deal with the unknown disturbances in vehicle systems, adaptive SMC (ASMC) was proposed to estimate the uncertain bound of the system parameters and disturbances [17]. However, the previously proposed AMSC strategies seldom considered the mitigation or elimination of the undesirable chattering effect, which makes the controller hard to implement in vehicle systems and easily causes the actuator abrasion. Also, the motion control of IA AV systems which have more actuators and sensors may involve various matched and mismatched disturbances. The previous AMSC strategies can hardly deal with that. Multivariable super-twisting control (STC) was proposed to generate the continuous controller in the presence of the matched disturbances to remove the chattering effect in SMC [18], [19], however, the main disadvantage of the multivariable STC is that it requires the prior knowledge of the boundaries of the disturbances, which are generally hard to identify or estimate in practice. Furthermore, the overestimation of the disturbance boundaries may easily yield to larger than necessary control gains, which could aggravate undesirable chattering effects.

To this end, this paper uses the DDAS angle to achieve lane keeping for AVs when the active steering motor completely fails, and make the following two contributions: 1) A novel adaptive multivariable STC approach is proposed to realize lane keeping control with chattering effect removed, in the presence of the multiple unknown and mismatched disturbances of the steering system; 2) In the definition of the sliding surface, a nonlinear function is designed to adaptively change the damping ratio of the closed-loop system, so as to improve the transient performance.

[1]Chuan Hu is with the Department of Systems Design Engineering, University of Waterloo, Waterloo, ON N2L 3G1, Canada. chuan.hu.2013@gmail.com

[2]Rongrong Wang is with the School of Mechanical Engineering, Shanghai JiaoTong University, Shanghai, 200240, China. wrr06fy@gmail.com

[3]The corresponding author Yechen Qin* is with the School of Mechanical Engineering, Beijing Institute of Technology, Beijing 100081, China, and also with the Department of Mechanical and Mechatronics Engineering, University of Waterloo, Waterloo, ON N2L 3G1, Canada. qinyechenbit@gmail.com

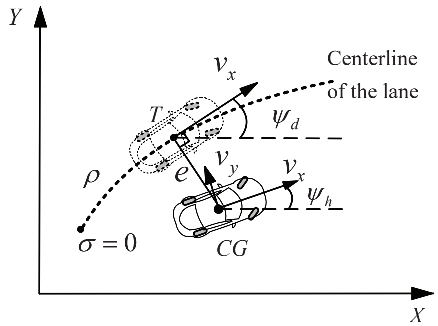

Fig. 1. Vehicle lane keeping kinematics model.

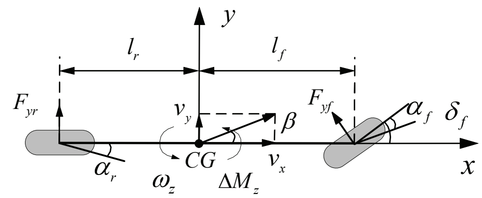

Fig. 2. 2 DoF model of the vehicle in the presence of sliding effects.

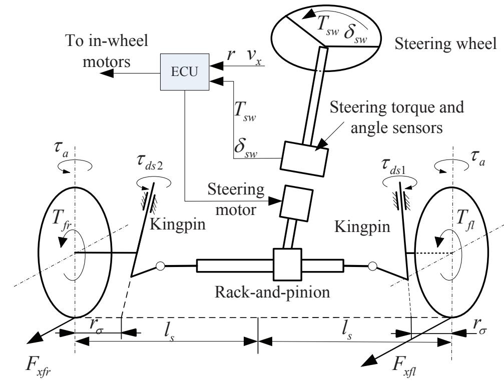

Fig. 3. Steering system model with the DDAS

II. Modelings of Lane Keeping and Vehicle Lateral Dynamics

A. Lane Keeping Model

The lane keeping model for AVs is shown in Fig. 1. The lateral offset e represents the distance from the vehicle center of gravity (CG) to its orthogonal projection (nearest) point T on the desired lane. The heading error ψ is the error between the real heading ψ_h and tangential direction of the desired lane ψ_d (i.e., $\psi = \psi_h - \psi_d$). v_x and v_y represent the longitudinal and lateral velocities, respectively. ω_z is the vehicle yaw rate, and we have $\dot{\psi}_h = \omega_z$. σ represents the curvilinear coordinate of the point T along the desired lane from a predefined initial position, and we have $\sigma \geq 0$, $\dot{\sigma} = d\sigma/dt$. $\rho(\sigma)$ is the curvature of the lane center line at the point T, which changes with the traveled distance σ. The lane curvature is assumed to be known in the lane keeping control of this study. Considering the small heading error, the lane keeping errors dynamics can be given by

$$\begin{cases} \dot{e} = v_x\psi + v_y, \\ \dot{\psi} = \omega_z - \rho(\sigma)\, v_x. \end{cases} \tag{1}$$

The control objective of the lane keeping control in (1) is to design appropriate control strategy to asymptotically and globally stabilize the lane keeping errors e and ψ such that the vehicle will track the road centerline asymptotically and maintain in the desired lane.

B. Modeling of Vehicle Lateral Dynamics and DDAS System

In this study, a 2-DoF (degree of freedom) "bicycle" model is used to obtain the vehicle lateral and yaw dynamics model, as shown in Fig. 2. The vehicle has a total mass m, and the inertia moment I_z about the yaw axis through the CG. The front and rear axles are located at distances l_f and l_r, from CG respectively. The sideslip angle and yaw rate are respectively denoted by β and ω_z. δ_f represents the front steering angle. It can assumed that v_x can be kept constant. The steering angle and tire slip angles are assumed sufficiently small, so the tires can be assumed to work in the linear region, and the vehicle handling dynamics equations can be derived as

$$\begin{cases} \dot{v}_y = \left(-v_x - \dfrac{l_f c_f - l_r c_r}{m v_x}\right)\omega_z - \dfrac{(c_f + c_r)}{m v_x} v_y + \dfrac{c_f}{m}\delta_f, \\ \dot{\omega}_z = \dfrac{\left(-{l_f}^2 c_f - {l_r}^2 c_r\right)}{v_x I_z}\omega_z + \dfrac{(l_r c_r - l_f c_f)}{I_z v_x} v_y + \dfrac{l_f c_f}{I_z}\delta_f + \dfrac{\Delta M_z}{I_z}, \end{cases} \tag{2}$$

where c_f and c_r are the generalized cornering stiffness of the front and rear tire, respectively. ΔM_z is the external yaw moment and $\Delta M_z = \Delta M_1 + \Delta M_2$, with ΔM_1 and ΔM_2 denoting the front and rear external yaw moments, respectively. ΔM_1 is the external yaw moment of the front axle, which generates the DDAS angle in faulty conditions. As the steering angle is assumed to be sufficiently small, it can be simplified as $\Delta M_1 \approx (F_{xfr} - F_{xfl})l_s$, where $F_{xfj}\ \ (j = l,\ r)$ respectively represents the longitudinal tire force of front-left and front-right wheels, and l_s is the half of the wheel track.

The configuration of the steering-by-wire (SbW) system for in-wheel-motor driven vehicles is shown in Fig. 3. Once the fault of the steering motor is detected, the DDAS mechanism will be activated to actuate the steering wheels. Based on the small slip-angle assumption with the brush tire model, the dynamics of the front steering angle of DDAS mechanism can be derived as [20]

$$\dot{\delta}_f = \frac{\kappa_1 c_f \delta_f}{b_{\text{eff}}} - \frac{\kappa_1 c_f l_f \Omega_z}{v_x b_{\text{eff}}} + \frac{\kappa_2 \Delta M_1}{b_{\text{eff}}} - \frac{\kappa_1 c_f v_y/v_x + \tau_f + J_{\text{eff}}\ddot{\delta}_f}{b_{\text{eff}}}, \tag{3}$$

where $\kappa_1 = l^2/3$ is a constant with l being the half of the tire contact length, $\kappa_2 = r_\sigma/l_s$ with r_σ being the scrub radius, b_{eff} represents the effective steering damping, J_{eff} represents the effective inertia torque, and τ_f represents the friction torque which combines the friction torques from the rack/pinion to the steering motor. Note that different from traditional vehicles, when the AFS system completely breaks down, the steering angle is not a control input any longer, but is converted into a vehicle state. The reason is that when the malfunction occurs, there is no steering wheel torque.

Denote the control input as $u = [u_1 \ u_2]^{\mathrm{T}}$, $u_1 = \Delta M_1$ $u_2 = \Delta M_2$. The second time-derivative of the steering angle $\ddot{\delta}_f$ can be assumed as a sufficiently small disturbance due to the physical meaning. The steering friction torque τ_f can also be assumed as a bounded disturbance. From (1) and (2), we can obtain the second-order time-derivatives of the lane keeping errors as

$$\begin{aligned}\ddot{e} = & \frac{(c_f + c_r)}{m}\psi - \frac{(c_f + c_r)}{mv_x}\dot{e} - \frac{(l_f c_f - l_r c_r)}{mv_x}\dot{\psi} \\ & + \frac{c_f}{m}\delta_f + \left(-v_x^2 - \frac{l_f c_f - l_r c_r}{m}\right)\rho,\end{aligned} \tag{4}$$

and

$$\begin{aligned}\ddot{\psi} = & \frac{(l_f c_f - l_r c_r)}{I_z}\psi + \frac{(l_r c_r - l_f c_f)}{I_z v_x}\dot{e} - \frac{\left({l_f}^2 c_f + {l_r}^2 c_r\right)}{v_x I_z}\dot{\psi} \\ & + \frac{l_f c_f}{I_z}\delta_f + \frac{1}{I_z}(u_1 + u_2) - \frac{\left({l_f}^2 c_f + {l_r}^2 c_r\right)}{I_z}\rho.\end{aligned} \tag{5}$$

After arrangement, we have the following state-space form

$$\begin{cases} \dot{x} = Ax + Bu + Ed + F(\rho), \\ y = C_1 x, \ z = C_2 x, \end{cases} \tag{6}$$

where $x = [e \ \psi \ \dot{e} \ \dot{\psi} \ \delta_f]^{\mathrm{T}}$, where $x_1 = [e \ \psi \ \dot{e}]^{\mathrm{T}}$ and $x_2 = [\dot{\psi} \ \delta_f]^{\mathrm{T}}$, and d is the disturbance defined as

$$d = -\frac{\tau_f + J_{\mathrm{eff}}\ddot{\delta}_f}{b_{\mathrm{eff}}}. \tag{7}$$

The system matrices can be given as

$$\begin{aligned} & A = \begin{bmatrix} A_{11} & A_{12} \\ A_{21} & A_{22} \end{bmatrix}, B = \begin{bmatrix} \mathbf{0}_{3\times 2} \\ B_2 \end{bmatrix}, E = \begin{bmatrix} \mathbf{0}_{3\times 1} \\ E_2 \end{bmatrix}, \\ & C_1 = \begin{bmatrix} I_{2\times 2} & \mathbf{0}_{2\times 3} \end{bmatrix}, \ C_2 = \begin{bmatrix} I_{4\times 4} & \mathbf{0}_{4\times 1} \end{bmatrix}, \\ & F(\rho) = \begin{bmatrix} F_1(\rho) & F_2(\rho) \end{bmatrix}^{\mathrm{T}}, \end{aligned} \tag{8}$$

with

$$A_{11} = \begin{bmatrix} 0 & 0 & 1 \\ 0 & 0 & 0 \\ 0 & \frac{(c_f + c_r)}{m} & -\frac{(c_f + c_r)}{mv_x} \end{bmatrix}, A_{12} = \begin{bmatrix} 0 & 0 \\ 1 & 0 \\ \frac{(l_r c_r - l_f c_f)}{mv_x} & \frac{c_f}{m} \end{bmatrix},$$

$$A_{21} = \begin{bmatrix} 0 & \frac{(l_f c_f - l_r c_r)}{I_z} & \frac{(l_r c_r - l_f c_f)}{I_z v_x} \\ 0 & \frac{\kappa_1 c_f}{b_{\mathrm{eff}}} & -\frac{\kappa_1 c_f}{v_x b_{\mathrm{eff}}} \end{bmatrix},$$

$$A_{22} = \begin{bmatrix} -\frac{\left({l_f}^2 c_f + {l_r}^2 c_r\right)}{v_x I_z} & \frac{l_f c_f}{I_z} \\ -\frac{\kappa_1 c_f l_f}{v_x b_{\mathrm{eff}}} & \frac{\kappa_1 c_f}{b_{\mathrm{eff}}} \end{bmatrix}, B_2 = \begin{bmatrix} \frac{1}{I_z} & \frac{1}{I_z} \\ \frac{\kappa_2}{b_{\mathrm{eff}}} & 0 \end{bmatrix},$$

$$E_2 = \begin{bmatrix} 0 \\ 1 \end{bmatrix}, \begin{cases} F_1(\rho) = H_1 f_1(\rho), \\ F_2(\rho) = [f_2(\rho) \ \ f_3(\rho)]^T, \end{cases}$$

where $H_1 = [0 \ 0 \ 1]^{\mathrm{T}}$, $f_1(\rho) = \left(-v_x^2 - \frac{l_f c_f - l_r c_r}{m}\right)\rho$, $f_2(\rho) = -\frac{\left({l_f}^2 c_f + {l_r}^2 c_r\right)}{I_z}\rho$, $f_3(\rho) = -\frac{\kappa_1 c_f l_f}{b_{\mathrm{eff}}}\rho$. Then the system can be reorganized as

$$\begin{cases} \dot{x}_1 = A_{11}x_1 + A_{12}x_2 + F_1(\rho), \\ \dot{x}_2 = A_{21}x_1 + A_{22}x_2 + B_2 u + E_2 d + F_2(\rho), \\ y = C_1 x, \ z = \mathrm{C}_2 x, \end{cases} \tag{9}$$

where $F_1(\rho)$ is a mismatched disturbance.

III. High-Performance Adaptive STC

Since the lane keeping and their time derivatives can be assumed bounded, a super-twisting observer [21] can be used to estimate the first derivative of the measured vector. In order to improve the transient performance of the closed-loop system, a novel nonlinear sliding surface $s(x)$ to counteract the mismatched disturbance $F_1(\rho)$ is defined as

$$s(x,t) = \Gamma x + \Lambda f_1(\rho), \tag{10}$$

where $\Gamma = [G \ \ 1]$ with $G = F - \varphi(z,r) A_{12}^{\mathrm{T}} P$, where Λ is a matrix to be designed, z is the controlled output, i.e., the lane keeping errors and their time derivatives. r is the reference vector of the controlled variable z, and is defined as $r = \mathbf{0}_{4\times 1}$. F is a matrix chosen to satisfy the condition that $A_{11} - A_{12}F$ has stable eigenvalues and its dominant poles have a very low damping ratio. It can be verified that pair $(A, \ B)$ in (6) is controllable, then one can conclude that the matrix pair $(A_{11}, \ A_{12})$ is also controllable. Therefore, for any given positive-definite and symmetric matrix W, there exists an unique positive-definite symmetric matrix P as the solution of the subsequent Lyapunov criterion

$$(A_{11} - A_{12}F)^{\mathrm{T}} P + P(A_{11} - A_{12}F) = -W. \tag{11}$$

$\varphi(z,r)$ in (10) is a negative function and is designed to be continuously differentiable with respect to z. It is used to gradually increase the damping ratio of the control system. $\varphi(z,r)$ is chosen as follows:

$$\varphi(z,r) = -\beta_0 \exp(-\rho_0 \|z - r\|^2), \tag{12}$$

where β_0 is a positive constant used to adjust the damping ratio. ρ_0 should be large enough to make $\varphi(z,r)$ has a tiny initial value. By designing appropriate SMC controller, the system will be forced to the sliding surface (10) such that $s(x,t) = 0$ is satisfied, which then yields

$$Gx_1 + x_2 + \Lambda f_1(\rho) = 0, \tag{13}$$

Combing (9) and (13), it yields that

$$\begin{aligned} \dot{x}_1 &= A_{11}x_1 + A_{12}x_2 + H_1 f_1(\rho) \\ &= [A_{11} - A_{12}G]\, x_1 + (-A_{12}\Lambda + H_1)\, f_1(\rho). \end{aligned} \tag{14}$$

To obtain Λ, we can partition A_{12} and H_1 as $A_{12} = [\mathbf{0}_{1\times 2} \ \bar{A}_{12}]^{\mathrm{T}}$, $H_1 = [0_{1\times 1} \ \bar{H}_1]^{\mathrm{T}}$, where

$$\bar{A}_{12} = \begin{bmatrix} 1 & 0 \\ -\frac{(l_f c_f - l_r c_r)}{mv_x} & \frac{c_f}{m} \end{bmatrix}, \bar{H}_1 = \begin{bmatrix} 0 \\ 1 \end{bmatrix} \tag{15}$$

Thus since one have $\Lambda = \bar{A}_{12}^{-1}\bar{H}_1$, where

$$\bar{A}_{12}^{-1} = \begin{bmatrix} 1 & 0 \\ \frac{(l_f c_f - l_r c_r)}{c_f v_x} & \frac{m}{c_f} \end{bmatrix}, \tag{16}$$

thus it yields that $\Lambda = [0 \;\; m/c_f]^{\mathrm{T}}$. Utilizing Λ the closed-loop system of x_1 (14) is converted into

$$\dot{x}_1 = [A_{11} - A_{12}G]\, x_1 = \left\{A_{11} - A_{12}\left[F - \varphi(z,r)\, A_{12}^{\mathrm{T}} P\right]\right\} x_1. \tag{17}$$

It can be observed from (13) that $x_1 = [e \;\; \psi \;\; \dot{e}]^{\mathrm{T}} \to 0 \Rightarrow x_2 = -\Lambda f_1(\rho)$, and also, according to the expression of Λ, we know $\dot{\psi} = 0$. Therefore, we have $e = 0, \;\; \psi = 0, \;\; \dot{e} = 0, \;\; \dot{\psi} = 0$, which then realizes the control objective of this paper. Based on (9), (11) and (17), a lemma is then presented to describe the convergence of x_1 as following:

Lemma 1 [22]: Consider the sliding surface (10) and closed-loop system (17), and suppose the aforementioned assumption is satisfied, when the trajectory of the system state is forced to reach the predefined sliding surface and remain on it thereafter, then the system state x_1 converges to the origin exponentially.

A. Adaptive Multivariable STC Design

Given the sliding surface is defined in the previous section, this section will develop the control law to drive the system sate to the sliding surface and stay on it. Taking the derivative of s according to (10) and (9) yields

$$\begin{aligned}
\dot{s} &= \left[-\frac{d\varphi(y,r)}{dt} A_{12}^{\mathrm{T}} P \;\; 0\right] \begin{bmatrix} x_1 \\ x_2 \end{bmatrix} \\
&\quad + \left[F - \varphi(y,r)\, A_{12}^{\mathrm{T}} P \;\; 1\right] \begin{bmatrix} \dot{x}_1 \\ \dot{x}_2 \end{bmatrix} + \Lambda \dot{f}_1(\rho) \\
&= \left[-\frac{d\varphi(y,r)}{dt} A_{12}^{\mathrm{T}} P \;\; 0\right] \begin{bmatrix} x_1 \\ x_2 \end{bmatrix} + \Lambda \dot{f}_1(\rho) \\
&\quad + G\left[A_{11}x_1 + A_{12}x_2 + H_1 f_1\right] + A_{21}x_1 \\
&\quad + A_{22}x_2 + B_2 u + \begin{bmatrix} f_2(\rho) \\ f_3(\rho) \end{bmatrix} + E_2 d.
\end{aligned} \tag{18}$$

The defined sliding surface is nonlinear and has continuously changing surface parameters. The desired control law should be chosen to force the system trajectory to move forwards the sliding surface and then remain on it thereafter from any initial condition. Also, as the bound of the disturbance d is unknown, the controller is expected to own a adaptive gains and remove the chattering effects. Inspired by [23] which proposed an adaptive-gain super-twisting sliding mode controller for second-order control systems, this work proposes an adaptive multivariable sliding mode controller with super-twisting algorithm to make the lane keeping errors converged to zero in finite time. The proposed control law is presented in the following theorem:

Theorem 1: Considering the nonlinear system (18), the sliding variable s and its derivative $\dot{s}$ will converge to zero in finite time if the sliding mode control law is designed as

$$\begin{aligned}
u = -B_2^{-1}\Bigg\{ &\left[-\frac{d\varphi(y,r)}{dt} A_{12}^{\mathrm{T}} P \;\; 0\right] x + \Lambda \dot{f}_1(\rho) \\
&+ G\left[A_{11}x_1 + A_{12}x_2 + F_1(\rho)\right] + A_{21}x_1 \\
&+ A_{22}x_2 + F_2(\rho) - \alpha_1 \frac{s}{\|s\|^{1/2}} + \varpi \Bigg\},
\end{aligned} \tag{19}$$

where $\dot{\varpi} = -(\beta_1/2)s/\|s\|$, with the adaptive gains α_1 and β_1 are as follows

$$\begin{cases} \dot{\alpha}_1 = \begin{cases} \omega_1 \sqrt{\gamma_1/2}, & \text{if} \;\; s > s_T \\ 0, & \text{if} \;\; s \le s_T \end{cases} \\ \beta_1 = 2\varepsilon_1 \alpha_1, \end{cases} \tag{20}$$

where $\omega_1, \; \gamma_1$, and ε_1 are some positive constants and s_T is a small threshold value.

Proof: Substitute the controller (19) into the system (18), it can be obtained that

$$\begin{cases} \dot{s} = -\alpha_1 \dfrac{s}{\|s\|^{1/2}} + \zeta, \\ \dot{\zeta} = -\dfrac{\beta_1}{2} \dfrac{s}{\|s\|} + E_2 \dot{d}, \end{cases} \tag{21}$$

where ζ denotes as $\zeta = \varpi + E_2 d$, and the adaptive gains α_1 and β_1 are provided in (20). It can be assumed that $||E_2\dot{d}|| \le \delta_m$ where δ_m is an unknown and bounded constant. To prove the stability of the closed-loop system (21), a Lyapunov function candidate is designed as

$$V = V_0 + \frac{1}{2\gamma_1}(\alpha_1 - \alpha_1^*)^2 + \frac{1}{2\gamma_3}(\beta_1 - \beta_1^*)^2, \tag{22}$$

where $V_0 = \vartheta^{\mathrm{T}} M \vartheta$, and the vector

$$\vartheta = \begin{bmatrix} \vartheta_1 & \vartheta_2 \end{bmatrix}^{\mathrm{T}} = \begin{bmatrix} \dfrac{s}{\|s\|^{1/2}} & \zeta \end{bmatrix}^{\mathrm{T}} \tag{23}$$

and

$$M = \begin{bmatrix} \lambda + 4\varepsilon_1^2 & -2\varepsilon_1 \\ -2\varepsilon_1 & 1 \end{bmatrix} \tag{24}$$

with α_1^*, β_1^* and γ_3 are some positive constants. Note that the matrix M is positive definite if $\lambda > 0$ and ε_1 are arbitrary positive constants. The time derivative of the Lyapunov function candidate V can be deduced as

$$\dot{V} = \dot{V}_0 + \tfrac{1}{\gamma_1}(\alpha_1 - \alpha_1^*)\,\dot{\alpha}_1 + \tfrac{1}{\gamma_3}(\beta_1 - \beta_1^*)\,\dot{\beta}_1 \tag{25}$$

where

$$\dot{V}_0 = \dot{\vartheta}^{\mathrm{T}} M \vartheta + \vartheta^{\mathrm{T}} M \dot{\vartheta} \le -\tfrac{1}{\|\vartheta\|^{1/2}} \vartheta^{\mathrm{T}} Q \vartheta, \tag{26}$$

where Q is a symmetric matrix computed from (21) and $||E_2\dot{d}|| \le \delta_m$ as

$$Q = \begin{bmatrix} q_{11} & q_{12} \\ q_{21} & q_{22} \end{bmatrix}, \tag{27}$$

with $q_{11} = \lambda\alpha_1 + 2\varepsilon_1(2\varepsilon_1\alpha_1 - \beta_1) + 4\varepsilon_1\delta_m, q_{12} = q_{21} = \left(\beta_1/2 - \varepsilon_1\alpha_1 - \lambda/2 - 2\varepsilon_1^2\right) - \delta_m, \;\; q_{22} = 4\varepsilon_1$. Here we define $\beta_1 = 2\varepsilon_1\alpha_1$ such that Q can be turned into a positive definite matrix, and if α_1 is chosen to satisfy

$$\alpha_1 > -\frac{\varepsilon_1(4\delta_m + 1)}{\lambda} + \frac{\left[2\delta_m + \lambda + 4\varepsilon_1^2\right]^2}{12\varepsilon_1\lambda}, \tag{28}$$

then it can be followed that the minimal eigenvalue of matrix Q satisfies $\lambda_{\min}(Q) \ge 2\varepsilon_1$. According to (26) and (28), it is easy to obtain that

$$\dot{V}_0 \le -\frac{\varepsilon_1 \lambda_{\min}^{1/2}(M)}{\lambda_{\max}(M)} V_0^{1/2}. \tag{29}$$

Define $\varepsilon_{\alpha_1} = \alpha_1 - \alpha_1^*$, $\varepsilon_{\beta_1} = \beta_1 - \beta_1^*$ and the positive constant ω_3, then (25) can be rewritten as

$$\begin{aligned}\dot{V} &\leq -\frac{\varepsilon_1 \lambda_{\min}^{1/2}(M)}{\lambda_{\max}(M)} V_0^{1/2} + \frac{1}{\gamma_1}\varepsilon_{\alpha_1}\dot{\alpha}_1 + \frac{1}{\gamma_3}\varepsilon_{\beta_1}\dot{\beta}_1 \\ &\leq -\frac{\varepsilon_1 \lambda_{\min}^{1/2}(M)}{\lambda_{\max}(M)} V_0^{1/2} - \frac{\omega_1}{\sqrt{2\gamma_1}}\left|\varepsilon_{\alpha_1}\right| - \frac{\omega_3}{\sqrt{2\gamma_3}}\left|\varepsilon_{\beta_1}\right| \\ &\quad + \frac{1}{\gamma_1}\varepsilon_{\alpha_1}\dot{\alpha}_1 + \frac{1}{\gamma_3}\varepsilon_{\beta_1}\dot{\beta}_1 + \frac{\omega_1}{\sqrt{2\gamma_1}}\left|\varepsilon_{\alpha_1}\right| + \frac{\omega_3}{\sqrt{2\gamma_3}}\left|\varepsilon_{\beta_1}\right|, \end{aligned} \tag{30}$$

In virtue of a well-known inequality $\left(x^2 + y^2 + z^2\right)^{1/2} \leq |x| + |y| + |z|$, for any real numbers x, y, and z, we can obtain

$$-\frac{\varepsilon_1 \lambda_{\min}^{1/2}(M)}{\lambda_{\max}(M)} V_0^{1/2} - \frac{\omega_1}{\sqrt{2\gamma_1}}\left|\varepsilon_{\alpha_1}\right| - \frac{\omega_3}{\sqrt{2\gamma_3}}\left|\varepsilon_{\beta_1}\right| \leq -\eta_0\sqrt{V}, \tag{31}$$

where $\eta_0 = \min\left\{\frac{\varepsilon_1 \lambda_{\min}^{1/2}(M)}{\lambda_{\max}(M)}, \omega_1, \omega_3\right\}$. Then (30) can be rewritten as $\dot{V} \leq -\eta_0\sqrt{V} + \xi$, where

$$\xi = -\left|\varepsilon_{\alpha_1}\right|\left(\frac{1}{\gamma_1}\dot{\alpha}_1 - \frac{\omega_1}{\sqrt{2\gamma_1}}\right) - \left|\varepsilon_{\beta_1}\right|\left(\frac{1}{\gamma_3}\dot{\beta}_1 - \frac{\omega_3}{\sqrt{2\gamma_3}}\right), \tag{32}$$

where the assumption that the adaptive gains $\alpha_1 < \alpha_1^*$ and $\beta_1 < \beta_1^*$ hold due to the adaptation law (20), and then it is followed that α_1 and β_1 are bounded. In order to achieve the finite-time convergence, we can choose the following adaption law of gains α_1 and β_1 as,

$$\begin{cases} \dot{\alpha}_1 = \omega_1\sqrt{\gamma_1/2}, \\ \dot{\beta}_1 = 2\varepsilon_1\dot{\alpha}_1 = \omega_3\sqrt{\gamma_3/2}, \end{cases} \tag{33}$$

where ε_1 should then be chosen as $\varepsilon_1 = \frac{\omega_3}{2\omega_1}\sqrt{\frac{\gamma_3}{\gamma_1}}$, after adopting the adaption law, we have $\dot{V} \leq -\eta_0\sqrt{V}$.

Note that to achieve finite-time convergence, α_1 must satisfy inequality (28), which can be satisfied at some time instant, as α_1 increases according to (20). After that, the finite-time convergence can be achieved in accordance with (20), and the sliding variable s and its derivative $\dot{s}$ can be converged to zero in finite time $t_s \leq \frac{2V^{1/2}(0)}{\eta_0}$. As soon as $s = \dot{s} = 0$ is guaranteed, there is no need to continue to increase α_1 and β_1, so the adaption law of α_1 is chosen as shown in (20). This completes the proof.

IV. Simulation Results

In this section, the simulation study is conducted on CarSim-Simulink platform with a full-car and high-fidelity vehicle model to verify the effectiveness of the proposed control strategy. The S-turn driving manoeuvre is investigated for the verification with a high longitudinal speed and the dry road condition. In the simulations, the active steering motor completely fails, which will then result in the exported steering torque becoming zero. Once this fault happens, the DDAS system will be actuated to generate a differential steering angle to steer the front wheels. The control objective is to maintain the lane keeping control using the DDAS angle and external yaw moment and guarantee high transient performance. The simulation verifies the lane keeping performance using the proposed controller when the vehicle is making a S-turn with a high speed ($v_x = 30$ m/s) on a high adhesion friction road ($\mu = 0.8$).

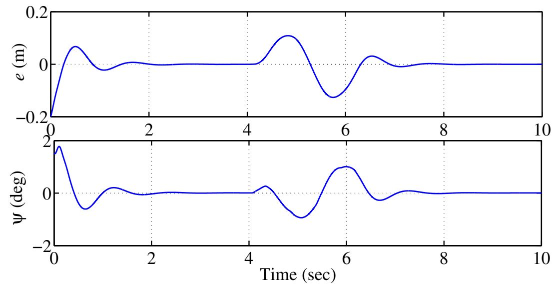

Fig. 4. Results of the lane keeping errors in the S-turn simulation

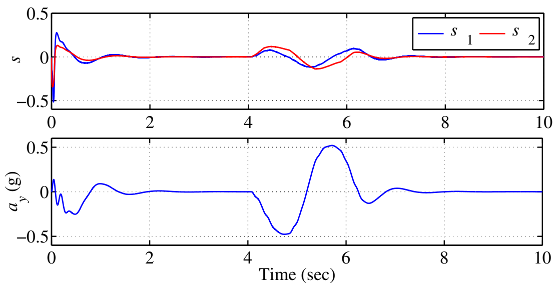

Fig. 5. Results of the sliding surface variables and lateral acceleration in the S-turn simulation

The results of the lane keeping errors are shown in Fig. 4. From the figure it is found the good and fast stabilization of the lane keeping errors is realized by the proposed DDAS mechanism and control strategy. As it is extremely dangerous to lose active steering power in tunings with high speed, the results of the S-turn prove that the DDAS mechanism is effective to provide emergence steering actuation, and can be used as a reliable redundancy steering actuator for emergency situations. The lateral offset and heading error are converged to zero simultaneously with small overshoots using the proposed approach. As the steering angle in this scenario (in highway) has smaller magnitude and shorter duration than that of the J-turn, the steady state error of the heading error will be smaller. The results of the sliding surface variables and lateral acceleration are shown in Fig. 5. The sliding variables are converged to zero rapidly and accurately, with small chattering and overshoots. The vehicle moves within the handling limit when the steering motor suddenly fails, that is, the lateral stability is guaranteed in this emergency situation.

The actual front steering angle and the external yaw moments are shown in Fig. 6. The front wheel shows a reasonable steering angle by using the differential torque and proposed approach, which can successfully complete the S-turn manoeuvre. The actuator inputs are controlled within the reasonable region. This proves the effectiveness of the DDAS mechanism in generating the emergency steering in

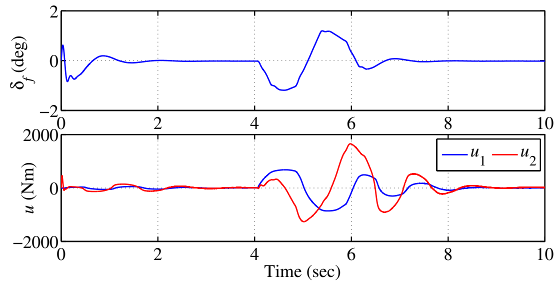

Fig. 6. Results of the steering angle and control inputs in the S-turn simulation

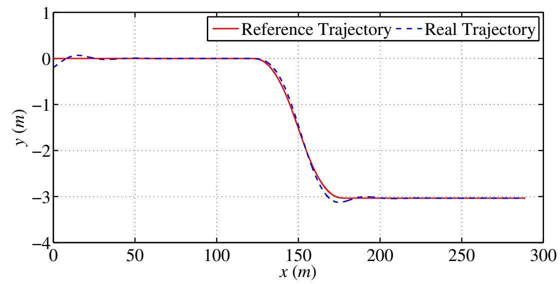

Fig. 7. Results of the global motion trajectory in the S-turn simulation

high speeds. It can also be found the steering angle and control inputs have small overshoots and chattering effects, showing the effectiveness of the proposed STC algorithm. The global S-turn trajectory are shown in Fig. 7, which has a high performance with smaller steady-state errors and overshoots. Therefore, it can be concluded that as an inherent and redundant steering actuator in FWIA electric vehicles, DDAS can be employed as a fault-tolerant steering actuator in emergency scenarios, and the proposed adaptive multivariable STC approach can effectually achieve robust lane keeping control with high performance considering the unknown mismatched disturbances.

V. Conclusion

This work investigates the lane keeping control for ADAS design of FWIA electric vehicles using the DDAS angle when the AFS system completely fails. DDAS is a inherent redundant steering actuator in independently actuated vehicles, generated by the yaw moment of the front axle. A novel adaptive multivariable STC algorithm is proposed to achieve the lane keeping control in the presence of the unknown unmatched disturbances, considering removing the chattering effect. To improve the transient performance, a nonlinear function is adopted in the sliding surface to adaptively change the damping ratio of the closed-loop system. High-fidelity CarSim-Simulink simulations with different driving scenarios have verified the effectiveness and robustness of the proposed approach with DDAS in yielding a high-performance, fast and accurate lane keeping control.

References

[1] C. Hu, H. Jing, R. Wang, F. Yan, and M. Chadli, "Robust H_∞ output-feedback control for path following of autonomous ground vehicles," *Mech. Syst. Signal Proc.*, vol. 70-71, pp. 414-427, Mar. 2016.

[2] X. Tang, W. Yang, X. Hu, and D. Zhang, "A novel simplified model for torsional vibration analysis of a series-parallel hybrid electric vehicle," *Mech. Syst. Signal Proc.*, vol. 85, pp. 329-338. Feb. 2017.

[3] Y. Huang, H. Wang, A. Khajepour, H. He, and J. Ji, "Model predictive control power management strategies for HEVs: A review," *J. Power Sources*, vol. 341, pp. 91-106, Feb. 2017.

[4] H. Wang, Y. Huang, A. Khajepour, H. He, and D. Cao, "A Novel Energy Management for Hybrid Off-road Vehicles without Future Driving cycles as A Priori," *Energy*, vol. 133, pp. 929-940, Aug. 2017.

[5] H. Wang, Y. Huang, A. Khajepour, "Cyber-Physical Control for Energy Management of Off-road Vehicles with Hybrid Energy Storage Systems," *IEEE-ASME Trans. Mechatron.*, 2018. DOI: 10.1109/TMECH.2018.2832019

[6] H. Wang, Y. Huang, A. Khajepour, T. Liu, Y. Qin, Y. Zhang, "Local Path Planning for Autonomous Vehicles: Crash Mitigation," *Proc. IEEE Intell. Vehicles Symp.*, Jun. 2018.

[7] Y. Qin, C. Xiang, Z. Wang, and M. Dong, "Road excitation classification for semi-active suspension system based on system response," *J. Vib. Control*, 1077546317693432, Feb. 2017.

[8] R. Wang, Y. Chen, D. Feng, X. Huang and J. Wang, "Development and performance characterization of an electric ground vehicle with independently actuated in-wheel motors," *J. Power Sources*, vol. 196, no. 8, pp. 3962-3971, Apr. 2011.

[9] C. Hu, R. Wang, and F. Yan "Output Constraint Control on Path Following of Four-Wheel Independently Actuated Autonomous Ground Vehicles," *IEEE Trans. Veh. Technol.*, vol. 65, no. 6, pp. 4033-4043, Jun. 2016.

[10] Y. Qin, C. He, X. Shao, H. Du, C. Xiang, and M. Dong, "Vibration mitigation for in-wheel switched reluctance motor driven electric vehicle with dynamic vibration absorbing structures," *J. Sound Vibr.*, vol. 419, pp. 249-267, Apr. 2018.

[11] Y. Qin, R. Langari, Z. Wang, C. Xiang, M. Dong, "Road Excitation Classification for Semi Active Suspension System with Deep Neural Networks," *J. Intell. Fuzzy Syst.*, vol. 33, no. 3, pp. 1907-1918, 2017.

[12] C. Hu, R. Wang, F. Yan, and H. R. Karimi, "Robust Composite Nonlinear Feedback Path-Following Control for Independently Actuated Autonomous Vehicles With Differential Steering," *IEEE Trans. Transport. Electrification*, vol. 2, no. 3, pp. 312-321, Sep. 2016.

[13] J. Wang, Q. Wang, L. Jin, and C. Song, "Independent wheel torque control of 4 WD electric vehicle for differential drive assisted steering," *Mechatronics*, vol. 21, no. 1, pp. 63-76, Feb. 2011.

[14] C. Hu, R. Wang, and F. Yan, "Integral sliding mode-based composite nonlinear feedback control for path following of four-wheel independently actuated autonomous vehicles," *IEEE Trans. Transport. Electrification*, vol. 2, no. 2, pp. 221-230, Jun. 2016.

[15] C. Hu, R. Wang, F. Yan, M. Chadli, Y. Huang, and H. Wang, "Robust path-following control for a fully actuated marine surface vessel with composite nonlinear feedback," *Trans. Inst. Meas. Control*, 0142331217727049, Sep. 2017.

[16] J. Li, A. Khajepour, Y. Huang, H. Wang, C. Tang, and Y. Qin, "A new coordinated control strategy for tracked vehicle ride comfort," *Proc. Inst. Mech Eng Pt K-J Multi-Body Dyn.*, 1464419317734950, Oct. 2017.

[17] Z. Sun, J. Zheng, Z. Man and H. Wang, "Robust control of a vehicle steer-by-wire system using adaptive sliding mode," *IEEE Trans. Ind. Electron.*, vol. 63, no. 4, pp. 2251-2262, Apr. 2016.

[18] I. Nagesh, C. Edwards, "A multivariable super-twisting sliding mode approach," *Automatica*, vol. 50, no. 3, pp. 984-988, Jan. 2014.

[19] J. A. Moreno, "On strict Lyapunov functions for some non-homogeneous super-twisting algorithms," *J. Frankl. Inst.*, vol. 351, no. 4, pp. 1902-1919, Apr. 2014.

[20] C. Hu, R. Wang, F. Yan, Y. Huang, H. Wang and C. Wei, "Differential Steering Based Yaw Stabilization Using ISMC for Independently Actuated Electric Vehicles," *IEEE Trans. Intell. Transp. Syst*, vol. 19, no. 2, pp. 627-638, Feb. 2018.

[21] A. Levant, "Higher-order sliding modes differentiation and output-feedback control," *Int. J. Control*, vol. 76, no. 9-10, pp. 924-941, 2003.

[22] S. Mobayen, D. Baleanu, "Stability analysis and controller design for the performance improvement of disturbed nonlinear systems using adaptive global sliding mode control approach," *Nonlinear Dyn.*, vol. 83, no. 3, pp. 1557-1565, Feb. 2016.

[23] Y. Shtessel, M. Taleb, and F. Plestan, "A novel adaptive-gain supertwisting sliding mode controller: Methodology and application," *Automatica*, vol. 48, no. 5, pp. 759-769, May 2012.